

N82 32065 D7 25

## FORMATION OF METALLIC AND METAL HYDROUS OXIDE DISPERSIONS

Egon Matijevic and R. S. Sapiieszko<sup>(a)</sup>

The formation, via hydrothermally induced precipitation from homogenous solution, of a variety of well-defined dispersions of metallic and hydrous metal in the conditions under which the particles are produced (e.g. pH and composition of the growth medium, aging temperature, rate of heating, or degree of agitation) can be readily discerned by following changes in the mass, composition, and morphology of the final solid phase. The generation of colloidal dispersions in the absence of gravity convection or sedimentation effects may result in the appearance of morphological modifications not previously observed in terrestrially formed hydrosols.

---

<sup>(a)</sup> Institute of Colloid and Surface Science and Department of Chemistry, Clarkson College of Technology

FORMATION OF METALLIC AND METAL HYDROUS OXIDE DISPERSIONS

by

Egon Matijevic<sup>1</sup> and R. S. Sapiieszko<sup>(a)</sup>

INTRODUCTION

Few families of inorganic compounds are as significant as metal (hydrous) oxides\*. These materials appear in nature as different minerals and ores and they are produced by hydrolytic corrosion of metals. In addition, metal hydrous oxides in various forms find numerous uses, such as pigments, catalysts, catalyst carriers, fillers, coatings, etc. Thus, it comes as no surprise that much work has been done on these compounds, both in terms of their preparation and characterization; nevertheless, relatively little is still known about the mechanism of formation of any of the metal oxides or hydroxides. This lack of knowledge is easily understood if one recognizes the complexity of the processes involved in the precipitation of such solids. For example, a minor change in pH can result in the formation of entirely different species in terms of chemical composition as well as of morphology. Equally important are the roles of other parameters, primarily of the temperature and of the nature of the anions in the solution in which the precipitation takes place. The latter can exercise a profound effect on the solid phase formed, even though the respective anions may not appear as constituent species of the precipitate. All the factors mentioned above (pH, temperature, anions) affect the complexation of the solutes which act as precursors to the nucleation of the metal hydrous oxides and which later determine their growth.

---

(a) Institute of Colloid and Surface Science and Department of Chemistry, Clarkson College of Technology, Potsdam, New York 13676

\* Metal (hydrous) oxide designation is taken here in a rather general way; it includes oxides, hydroxides, hydrated oxides, oxyhydroxides, etc.

The sensitivity of the described precipitation processes explains the poor reproducibility usually encountered in the studies of metal hydrous oxide formation. It also accounts for the finding that the resulting solids are mostly ill defined in shape and polydisperse.

Over the past few years we have succeeded in the preparation of colloidal dispersions of a number of metal hydrous oxides consisting of particles exceedingly uniform in size and shape (1). Such sols can be repeatedly obtained by relatively simple procedures and, as one would expect, the morphology, chemical composition, and other characteristics of the precipitates depend strongly on the experimental conditions. The reproducibility in the generation of well defined suspensions makes the elucidation of the chemical formation mechanisms possible. In order to accomplish the latter aim, the knowledge of the composition of all species in solution, in which the solid phase is formed, and particularly of the complexes containing the metal ion which is the major constituent of the precipitate, is implied. The task in obtaining this information is by no means easy. The monodispersed sols can also be employed in studies of various phenomena, such as in adsorption, adhesion, heterocoagulation, color determination, to mention a few.

In this presentation, an overview of the author's program in metal hydrous oxides will be offered with examples in the following areas of research:

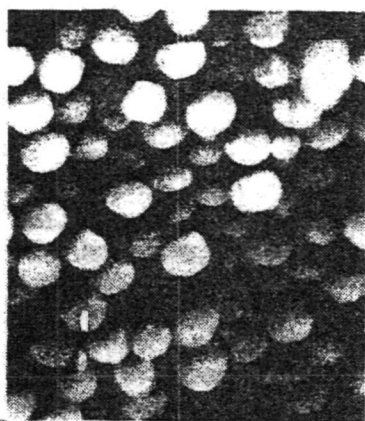
- a. Preparation of monodispersed sols.
- b. Mechanism for formation.
- c. Characterization of the particulate matter.
- d. Interactions with solutes.
- e. Interactions with other particles.
- f. Adhesion.

PREPARATION OF MONODISPERSED SOLS OF METAL HYDROUS OXIDES

If uniform particles are to be obtained from a solution in which the precipitating components are continuously generated, secondary nucleation must be avoided. This condition implies that, upon reaching the critical supersaturation leading to the burst of nuclei, the rate of crystal growth must exceed the rate of nuclei formation. In the case of systems studied in this work, complexes of metal ions with hydroxyls, and often with other anions, are the precursors to the solid phase separation. Thus, hydroxylation is the controlling step, which will determine the nature of the final product. The usual procedure of adding base leads to local supersaturations and, consequently, to poorly defined stages of nucleation and particle growth. As a result the produced solids are irregular in shape and of broad size distributions.

Hydroxylation is greatly accelerated with temperature, depending on the metal and on the temperature of aging, hydrolyzed metal ion complexes may form in solutions of various degrees of acidity. Thus, it is possible to regulate the rate of complex formation in an aqueous solution of metal salts by proper adjustment of pH and temperature. Once the solution becomes supersaturated in the constituent species of a given metal hydrous oxide, the nucleation occurs. Further aging at a convenient temperature will continue to produce the precipitating complexes which, assuming a proper rate of their generation, are consumed in particle growth. Consequently, no secondary nucleation will take place, and a uniform uptake of the constituent species by the existing primary particles yields a monodispersed sol.

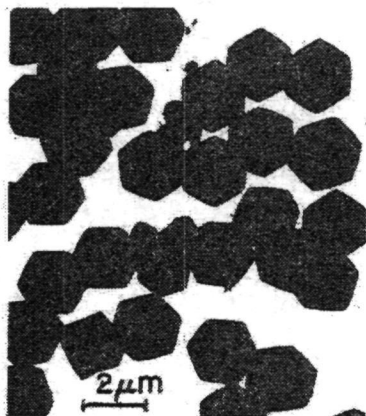
The chemical composition of the solid will strongly depend on the nature of the complex solutes produced on aging. In this respect the anions play a dominant role. In some cases well defined stoichiometric species form which include one or more hydroxyl and negatively charged ions, whereas in other cases the anions may cause condensation of hydrolysis products into polynuclear solutes of different



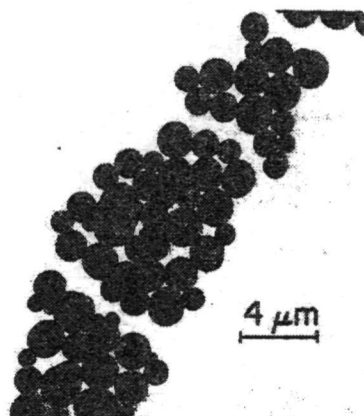
a



b



c



d

Fig. 1. Scanning and transmission electron micrographs of particles precipitated from various ferric salt solutions. (a) Hematite,  $\alpha\text{-Fe}_2\text{O}_3$  (solution 0.0315 M in  $\text{FeCl}_3$  and 0.005 M in  $\text{HCl}$  aged for 2 weeks at  $100^\circ\text{C}$ ). (b)  $\beta\text{-FeOOH}$  (solution 0.27 M in  $\text{FeCl}_3$  and 0.01 M in  $\text{HCl}$  aged for 24 hr at  $100^\circ\text{C}$ ). (c) Ferric basic sulfate  $\text{Fe}_3(\text{OH})_5(\text{SO}_4)_2 \cdot 2\text{H}_2\text{O}$  (solution 0.18 M in  $\text{Fe}(\text{NO}_3)_3$  and 0.32 M in  $\text{Na}_2\text{SO}_4$  aged for 2 hr at  $98^\circ\text{C}$ ). (d) Ferric phosphate,  $\text{FePO}_4$  (solution 0.0038 M in  $\text{FeCl}_3$  and 0.24 M in  $\text{H}_3\text{PO}_4$  at pH 1.86 aged for 20 min at  $100^\circ\text{C}$ ).

degrees of complexity. As a result the precipitated particles from solutions of different salts of the same metal ion may have different composition and structure.

To illustrate the above described situations in Figure 1 are given electron micrographs of four different systems, all precipitated by aging acidified ferric salt solutions. The scanning electron micrograph 1a shows spherical particles of hematite ( $\alpha\text{-Fe}_2\text{O}_3$ ) obtained by aging a solution 0.0315 M in  $\text{FeCl}_3$  and 0.005 M in HCl for 2 weeks at  $100^\circ\text{C}$  (2), whereas 1b is a transmission electron micrograph of  $\beta\text{-FeOOH}$  particles generated in solution 0.27 M in  $\text{FeCl}_3$  and 0.01 M in HCl heated at  $100^\circ\text{C}$  for 24 hr. Figure 1c represents submicron alunite type crystals of the composition  $\text{Fe}_3(\text{OH})_5(\text{SO}_4)_2 \cdot 2 \text{H}_2\text{O}$  which formed on aging at  $98^\circ\text{C}$  for 2 hr a solution 0.18 M in  $\text{Fe}(\text{NO}_3)_3$  and 0.32 M in  $\text{Na}_2\text{SO}_4$  (3). Finally, Figure 1d shows particles obtained on heating for 20 min at  $100^\circ\text{C}$  a solution which was 0.0038 M in  $\text{FeCl}_3$ , 0.24 M in  $\text{H}_3\text{PO}_4$  with NaOH added to adjust the pH to 1.86. The chemical analysis of these particles gave a composition consistent with  $\text{FePO}_4$ .

The four examples show that in the presence of chloride ions, under rather similar conditions, two entirely different sols are generated in terms of chemical composition and particle morphology (Figures 1a and b). The solid  $\beta\text{-FeOOH}$  contained considerable amounts of chloride ions when freshly prepared, but these anions could be removed by repeated washing with water without any apparent change in particle size or shape. On the other hand, solids formed on heating ferric salt solutions in the presence of sulfate ions consist of stoichiometrically stable and structurally well defined basic ferric sulfates. Finally, no detectable amounts of hydroxyl ligands are found in the systems precipitated as described above from aged solutions in the presence of phosphate ions. The resulting ferric phosphate redissolves on cooling.

The four different dispersions shown in Figure 2 were obtained by aging acidified aluminum salt solutions. Again the anions play an essential role.

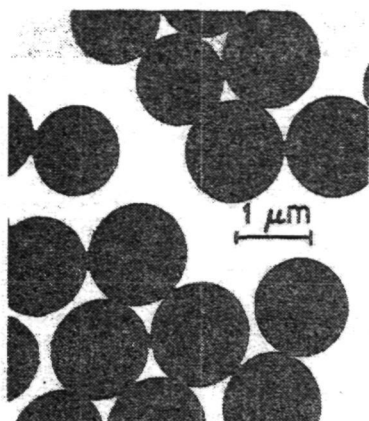
The perfect spheres (Figure 2a) were generated on heating aluminum sulfate solutions ( $2 \times 10^{-3}$  M) for 48 hr at  $97^{\circ}\text{C}$  (initial pH 4.0). The precipitate contained a considerable amount of sulfate ions, but these anions were readily leached out by rinsing the solids with water yielding pure amorphous aluminum hydroxide particles without change in shape (4). Heating at the same temperature for 20 hr a solution which was 0.050 M each in  $\text{Al}(\text{NO}_3)_3$  and  $\text{Na}_2\text{HPO}_4$  and 0.035 M in  $\text{HNO}_3$  (initial pH of the mixture being 2.0) gave also spherical particles (Figure 2b) but the X-ray and chemical analysis identified the solids to be consistent with the composition of the mineral variscite,  $\text{AlPO}_4$ . Scanning electron micrographs (2c and d) show two unusual morphologies of boehmite, obtained by aging of aluminum chloride (0.0050 M  $\text{AlCl}_3$ ) and aluminum perchlorate (0.0030 M  $\text{Al}(\text{ClO}_4)_3$ ) solutions, respectively, at  $125^{\circ}\text{C}$  for 12 hr (5).

Again, it is clearly demonstrated that rather different, yet quite uniform colloidal metal oxide dispersions, can be prepared by homogeneous precipitation of different salt solutions in which different anions have a profound effect on the properties of the solid formed.

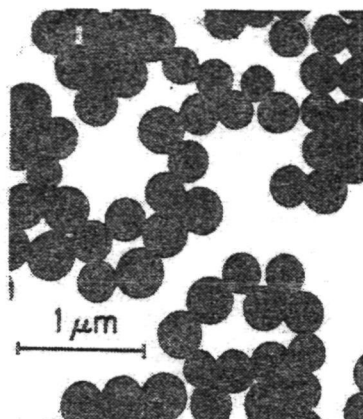
As a last example, Figure 3 gives a transmission electron micrograph and a replica of  $\text{Co}_3\text{O}_4$  particles which have a spinel structure. The significant finding is that such systems are formed on heating at  $100^{\circ}\text{C}$  of cobalt(II) salt solutions in oxygen or air only in the presence of acetate ions. No precipitate was obtained when, under otherwise identical conditions, the sulfate, chloride, perchlorate, or nitrate salts of cobalt(II) were aged.

Many more monodispersed sols of different hydrous metal oxides, involving those of chromium (6,7) copper (8), titanium (9), and other metals, have now been prepared following similar procedures.

ORIGINAL PAGE  
BLACK AND WHITE PHOTOGRAPH



a



b



c



d

Fig. 2. Transmission and scanning electron micrographs of particles precipitated from various aluminum salt solutions. (a) Amorphous aluminum hydroxide (solution 0.0020 M in  $\text{Al}_2(\text{SO}_4)_3$ , pH 4.0 aged for 48 hr at  $97^\circ\text{C}$ ). (b) Variscite,  $\text{AlPO}_4$  (solution 0.050 M in  $\text{Al}(\text{NO}_3)_3$  and  $\text{Na}_2\text{HPO}_4$  and 0.035 M in  $\text{HNO}_3$  aged for 20 hr at  $97^\circ\text{C}$ ). (c) and (d) Boehmite,  $\alpha\text{-AlOOH}$  (solutions of 0.0050 M in  $\text{AlCl}_3$  and 0.0030 M in  $\text{Al}(\text{ClO}_4)_3$ , respectively, aged for 12 hr at  $125^\circ\text{C}$ ).



## MECHANISM OF METAL HYDROUS OXIDE FORMATION

The examples in the preceding section clearly show that it is necessary to know the composition of the solution in terms of the nature and of the concentration of all complexes if one is to explain the chemical processes in homogeneous precipitation of metal hydroxides. Unfortunately, such information is not always available, particularly for solutions at higher temperatures. Thus, one has no choice but to determine the composition of the different solutes under the actual conditions of the solid phase formation.

Until recently no substantiated mechanisms on metal hydroxide formation have been available (10). Using the monodispersed sols it was possible to develop a better understanding of the essential processes in the generation of chromium hydroxide (11,12), titanium dioxide (9), and ferric basic sulfates (13). In all these cases the particles formed in the presence of sulfate ions, but the role of these anions was quite different in each system.

Thus, in solutions containing chromium and sulfate ions solid chromium basic sulfate precursor precipitates first, which acts as a heterogeneous nucleating material for the amorphous chromium hydroxide (11). An application of the Nielsen's chromal analysis showed that the particles grow via surface reaction which involves polynuclear layer growth (12).

In the highly acidic solutions of titanium salts, sulfate ions bind the titanium(IV) ions into solute complexes, which on prolonged aging at elevated temperatures slowly decompose. These species act as a reservoir for the titanium ions; on decomplexation they hydrolyze and precipitate.

Finally, in solutions containing ferric and sulfate ions at low pH, well defined monomeric and dimeric solute hydroxy and sulfato complexes of iron(III) form, giving crystals of fixed stoichiometric composition (13).

ORIGINAL PAGE  
BLACK AND WHITE PHOTOGRAPH

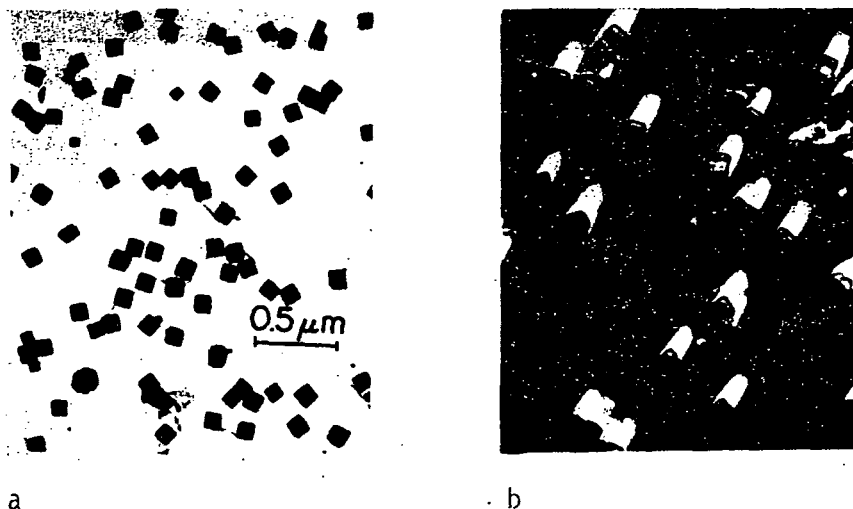


Fig. 3. Electron micrograph and a replica of  $\text{Co}_3\text{O}_4$  spinel particles obtained by heating a 0.010 M Co(II)-acetate solution for 4 hr at 100 C.

The role of chloride ions in the precipitation of different ferric hydroxous oxides has not been explained yet, but the work on the chloro-ferric complexes in acidic solutions, which is presently carried out in our laboratory, may shed light on the findings that a relatively small variation in conditions not only yield particles of different morphologies, but also of entirely different chemical compositions.

#### CHARACTERIZATION OF MONODISPersed METAL HYDROUS OXIDE SOLS

Depending on application, the characterization of colloidal particles may take many forms. In this review, only two properties will be discussed: surface charge and magnetism.

##### Surface Charge

Owing to the nature of the stabilizing species ( $\text{OH}^-$ ,  $\text{H}^+$ ) the surface charge of any metal hydroxous oxide is strongly pH dependent. Furthermore, the

electrokinetic point of zero charge (isoelectric point, i.e.p.) varies not only with the constituent metal, but also with the composition of its hydrous oxides. As a matter of fact, the reported values for the i.e.p. for apparently the same materials differed by several units in pH (14). For example, the literature data for the i.e.p. of synthetic titanium dioxide range from pH 2.6 to 7.3, whereas for a very pure sample of  $TiO_2$  it was found to be between 4.5 and 5.2 (15). In another example, the cubic  $Co_3O_4$  particles illustrated in Figure 3 show an i.e.p. at pH 5.4 (16); a considerably higher value of 11.4 was reported for a Co(II,III) oxide by Tewari and Campbell (17).

Since the isoelectric point defines the pH below which the particles are positively charged and above which they are negatively charged, this property of a metal hydrous oxide is essential in considering the sol stability, particle adhesion, heterocoagulation with other particles, and interactions with different solutes.

Figure 4 gives the electrokinetic mobility data of four aluminum hydroxide sols as a function of pH. Three of these curves refer to systems illustrated in Figure 2. The interesting finding is that the largest difference in the mobility curves is for two amorphous spherical particles prepared by aging aluminum sulfate solutions. The lower values of the i.e.p. is for the sol, as directly generated (diamonds), whereas the higher value is for the same sol from which the sulfate ions were removed by repeated rinsing with water (triangles). This example shows that anionic "impurities" have a pronounced effect on the surface charge characteristics of metal hydrous oxides. Obviously, the discrepancies in many reported data may be due to similar causes.

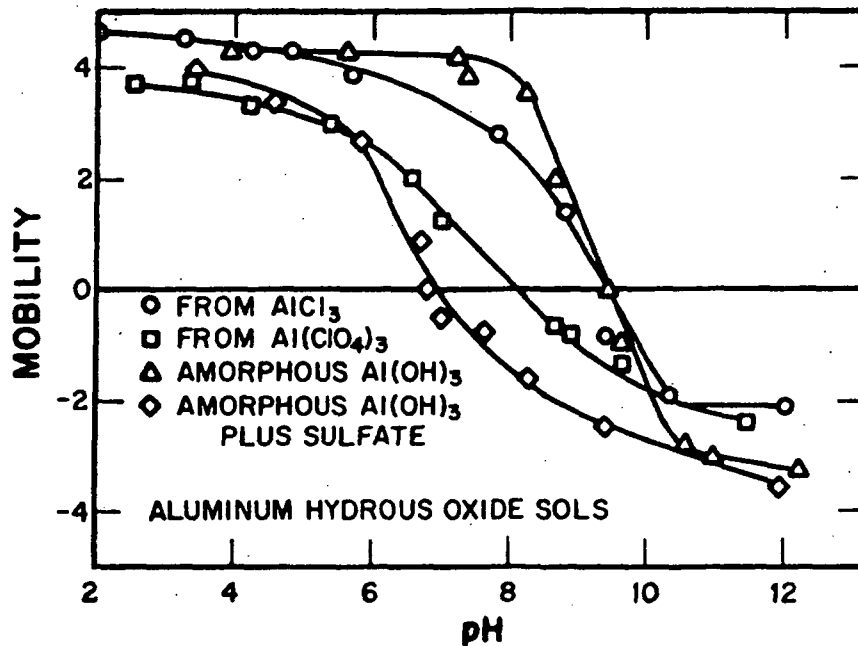


Fig. 4. Electrokinetic mobilities ( $\mu\text{m}/\text{sec}/\text{V}/\text{cm}$ ) as a function of pH of four different colloidal aluminum hydroxide oxides as illustrated in Figure 1c (○), 1d (□), 1a (△), and the same particles as shown in 1a from which sulfate ions were removed by leaching (◇).

### Magnetism

It is well known that magnetic properties of different (hydrated) oxides of a given metal strongly depend on their composition. Much less well understood is the relationship between various types of magnetism and the shape of the particles of the same chemical composition or of the materials having the same chemical composition and shape but different particle size. The monodispersed metal hydroxide oxides lend themselves exceedingly well for the investigation of magnetic properties as a function of various parameters.

Figure 5 shows the magnetization as a function of applied magnetic field for nearly spherical  $\alpha\text{-Fe}_2\text{O}_3$  particles (30-40 nm modal diameter at 298<sup>0</sup>K). It was suggested that hematite particles of this size should be in the antiferro-

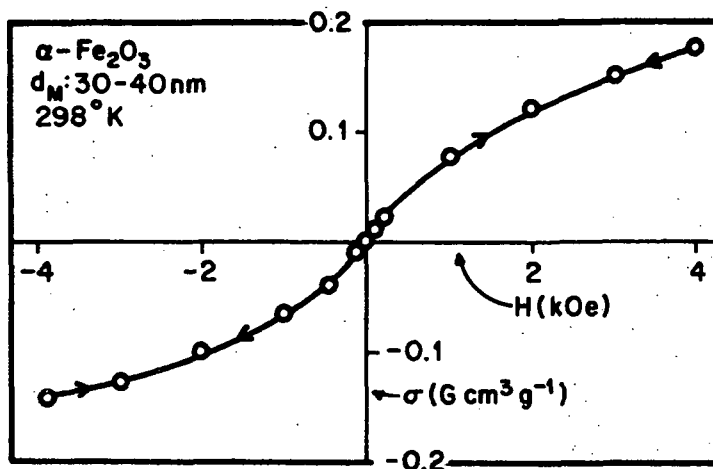


Fig. 5. Magnetization at  $298^\circ\text{K}$  as a function of applied field of spherical  $\alpha\text{-Fe}_2\text{O}_3$  particles having modal diameters of 30-40 nm.

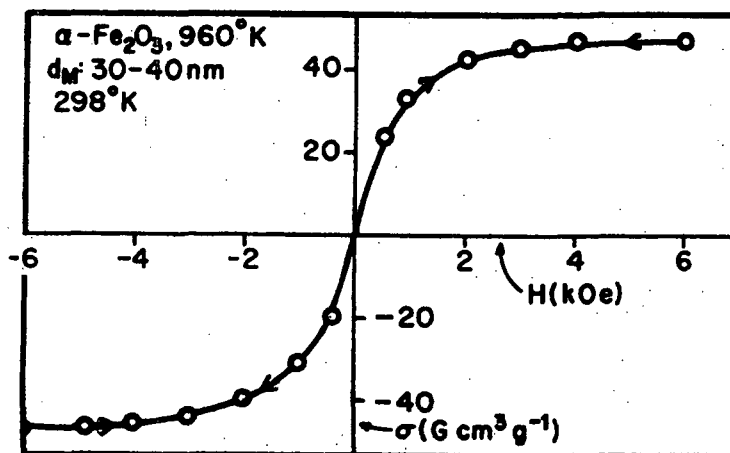


Fig. 6. Magnetization at  $298^\circ\text{K}$  as a function of applied magnetic field of spherical  $\alpha\text{-Fe}_2\text{O}_3$  particles having modal diameters of 30-40 nm after heat treatment at  $960^\circ\text{K}$  in a He atmosphere of 500 torr.

magnetic state (18). Thus, the  $\sigma$  vs H plot should exhibit some hysteresis. Within the experimental error no hysteresis is seen and the curve is typically S-shaped, characteristic of pure superparamagnetism (possibly in coexistence with weak ferromagnetism). This observation would suggest that the proposed relationship of the magnetic states to particle size (18) for  $\text{Fe}_2\text{O}_3$  systems may not be correct.

Heating the same hematite particles at high temperatures ( $960^\circ\text{K}$ ) in the helium atmosphere of 500 torr drastically alters the magnetic properties of  $\alpha\text{-Fe}_2\text{O}_3$  (Figure 6), although little change could be observed with respect to particle size and shape. The high  $\sigma$  values indicate the presence of ferromagnetic components, presumably  $\text{Fe}_3\text{O}_4$  or  $\gamma\text{-Fe}_2\text{O}_3$ , in these particles. Obviously, the crystallinity of the solids must have been affected by the heat treatment.

#### INTERACTIONS WITH SOLUTES

It is well known that the surfaces of hydrous metal oxides are rather reactive, i.e. various molecular or ionic species adsorb on such solids from aqueous solutions. The interfacial processes depend on the pH, since the latter is the factor controlling the surface charge. It is important to note that the opposite charge between the adsorbent and the adsorbate is not a sufficient condition for adsorption. The electrostatic attraction will only facilitate the approach of the solute species to the particle surface; other forces are needed to keep them at the interface. These forces may be hydrogen bond or other types of bindings (such as chelation), surface precipitation, etc. It is the ability of the constituent metal ions and of the potential determining species to interact with a variety of solutes that make metal hydrous oxide surfaces so reactive.

Two examples to be given here deal with the interaction of monodispersed, spherical, amorphous chromium hydroxide particles with aspartic acid and of crystalline rod-like  $\beta\text{-FeOOH}$  particles with ethylenediamine tetraacetic acid (EDTA).

ORIGINAL PAGE IS  
OF POOR QUALITY

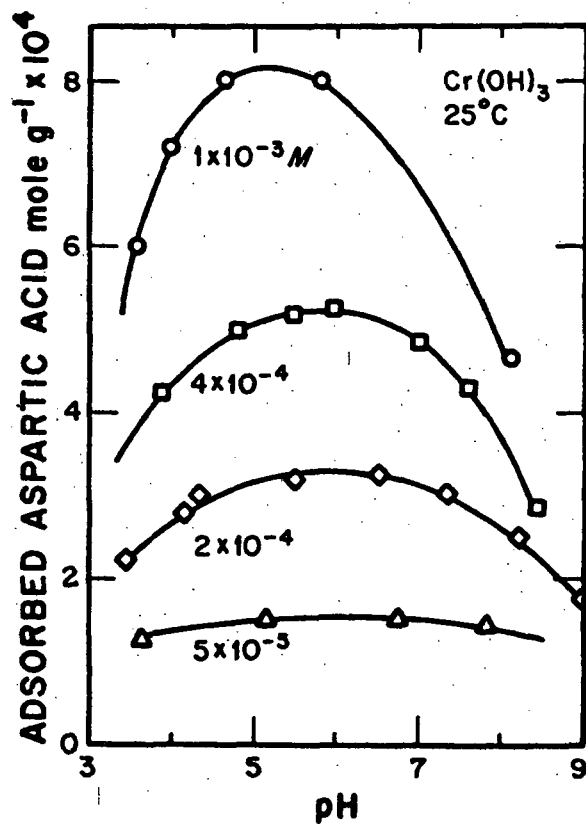


Fig. 7. The total amount of aspartic acid sorbed on spherical chromium hydroxide particles (modal diameter 350 nm) as a function of pH using different initial concentrations of aqueous solutions of the amino acid.

Figure 7 gives the total amount of aspartic acid sorbed on a chromium hydroxide sol having particles of a modal diameter of 350 nm as a function of pH using different initial concentrations of the solute. Analogous measurements showed that at 90°C the adsorbed amounts are considerably higher (19). The pH effect is obviously due to the charge on the solid. The i.e.p. of the used sol is at pH ~ 8.5 and little uptake of aspartic acid was observed above this pH value. It is evident that opposite charges of the adsorbent and adsorbate are needed to bring about the interaction.

The significant finding is that the amounts of the amino acid taken up by the metal hydroxide are approximately four orders of magnitude higher than the quantities calculated on the basis of monolayer adsorption assuming geometric surface areas of the spherical adsorbent particles. The obvious conclusion is that the major fraction of the aspartic acid molecules is absorbed in the interior of the adsorbent, which presumes that the amorphous chromium hydroxide is permeable to this amino acid. The absorption seems to be due either to chelation or to coordination of chromium ions with aspartic acid molecules. The much stronger uptake of these solute species at higher temperature supports the suggested chemisorption mechanism.

Contrary to the findings with aspartic acid, the same chromium hydroxide sol did not adsorb any measurable quantities of tryptophan. The latter is a larger molecule with a stronger aromatic (hydrophobic) character; its monocarboxylate nature (as distinguished from the dicarboxylic aspartic acid) precludes chelate formation by the carboxyl groups only.

The amount of EDTA adsorbed on  $\beta$ -FeOOH is also pH dependent and the uptake decreases strongly with increasing pH (Figure 8). The area per Fe atom in  $\beta$ -FeOOH, calculated from the crystal structure of this solid, is  $27 \text{ \AA}^2$ , and the



ORIGINAL PAGE IS  
OF POOR QUALITY

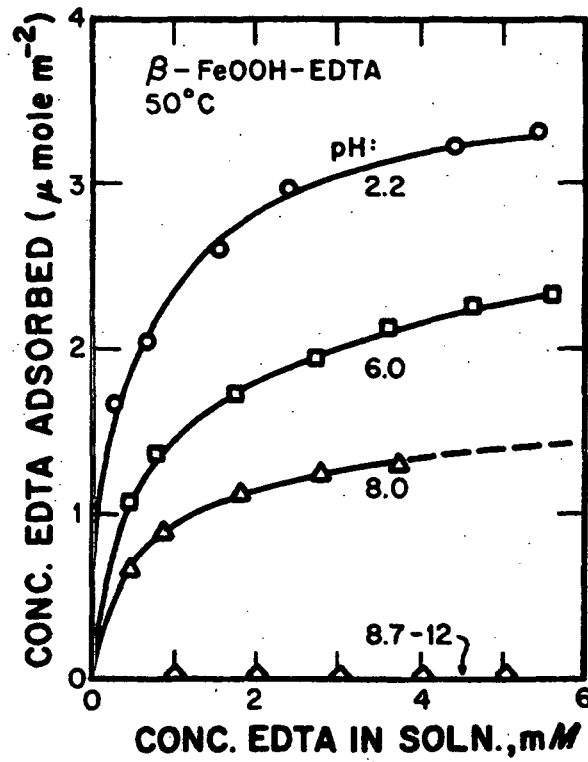


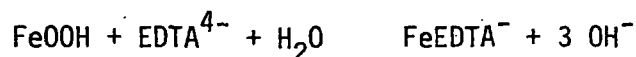
Fig. 8. Adsorption isotherms at 50°C for EDTA on  $\beta$ -FeOOH consisting of rod-like particles with an average length of 1  $\mu$ m and a width of 0.3  $\mu$ m. Each curve is for a different pH value.

area per ligand molecule at the condition of maximum adsorption at pH 2.8 (at 25°C), as calculated from the corresponding adsorption isotherm and the BET specific surface area of the ferricoxyhydroxide, is  $33 \text{ \AA}^2$ . The latter value is in reasonable agreement with the estimated cross-sectional area of the EDTA molecule, which indicates that at saturation a monomolecular layer is formed based on a Fe:EDTA interfacial complex of 1:1. The surface complexation is further supported by the value of the free energy of adsorption, which was found to be  $\Delta G_{\text{ads}}^0 = -9 \text{ kcal/mole}$  (20).

It was of special interest to investigate if the interaction of EDTA with the same  $\beta\text{-FeOOH}$  was accompanied by dissolution of some of the oxyhydroxide. Figure 9 is a plot of the amount of ferric ions released as a function of pH in the absence of EDTA and in the presence of three different concentrations of this chelating agent. A very pronounced maximum is observed. At lower pH values, at which considerable adsorption takes place, the release of ferric ions is rather small; the dissolution is inhibited by the surface complexation of lattice ferric ions with the organic ligand.

The maximum dissolution of ferric ions is over the pH range 8-10. Under these conditions no adsorption takes place. Partial dissolution of particles yields positively charged ferric hydrolysis products ( $\text{Fe}(\text{OH})_2^+$ ,  $\text{FeOH}^{2+}$ ,  $\text{Fe}_2(\text{OH})_2^{4+}$ ) which react with EDTA anions and, thus, enhance further release of ferric ions from the solid  $\beta\text{-FeOOH}$ .

Finally, at the highest pH values (> 12), the complete inhibition of the dissolution can be understood, if one considers that the reaction



is strongly shifted to the left.

The two examples offered clearly illustrate the important role of specific interactions between a solid and a solute resulting in entirely different behavior of different systems.

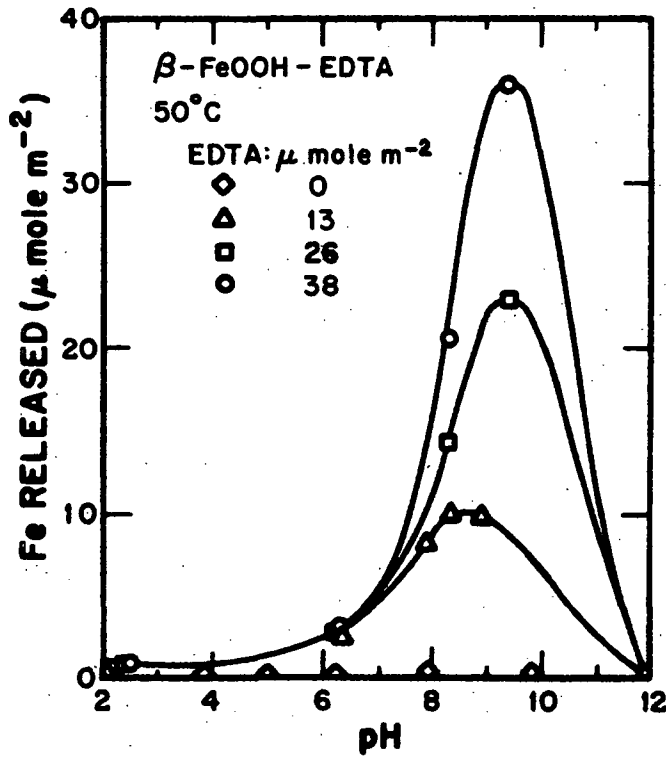


Fig. 9. Solubility of  $\beta$ -FeOOH (expressed as released iron) in the absence and in the presence of EDTA in different concentrations as a function of pH at 50°C.

## INTERACTIONS OF METAL HYDROUS OXIDES WITH OTHER PARTICULATE MATTER

### Heterocoagulation

Most of the colloid stability studies have been carried out with single systems, preferably monodispersed sols, such as polymer latexes. Yet, by far a majority of the naturally occurring dispersions, or those used in various applications, consists of mixed type particles, which may vary in composition, size, shape, and other phenomena, which implies stability of systems containing dissimilar suspended solids.

In order to apply the theoretical analysis it is necessary to work with spherical particles of known size, potential, and specific attraction characteristics. In addition, the stability of such mixed systems depends on the ratio of the particle number concentrations as well as on the ionic composition of the suspending media.

Monodispersed spherical metal hydrous oxide sols are particularly suitable for the study of interactions between unlike particles, because the necessary parameters can be experimentally determined. A comprehensive investigation was carried out with a binary system consisting of a polymer (polyvinyl chloride, PVC) latex stabilized with sulfate ions and spherical chromium hydroxide particles (21). The advantage of such a combination is that changing pH affects little the surface potential of the latex, whereas the metal hydroxide particles not only undergo a change in this quantity, but the sign of the charge can be reversed. The obtained data showed that excellent qualitative agreement existed between the experimental results and the theoretical calculations for dispersions of these two colloids.

To illustrate the effects of interactions in a mixed system, the stability ratios of sols consisting of spherical aluminum hydroxide particles (4) having a modal diameter of 570 nm and of a polystyrene latex (PSL, modal diameter 380 nm)

stabilized by sulfate ions will be given. The rate of coagulation was followed by means of laser light scattering at a low angle ( $\theta = 5^\circ$ ). Figure 10 is a plot of the total stability ratio,  $W_T$ , defined as

$$1/W_T = (n_1^2/W_{11}) + (n_2^2/W_{22}) + (2n_1n_2/W_{12}) \quad (1)$$

where  $W_{11}$  and  $W_{22}$  are the homocoagulation stability ratios for aluminum hydroxide and the latex, respectively, and  $W_{12}$  is the heterocoagulation stability ratio.  $n_1$  and  $n_2$  are the primary particle number fractions of the two dissimilar particles.

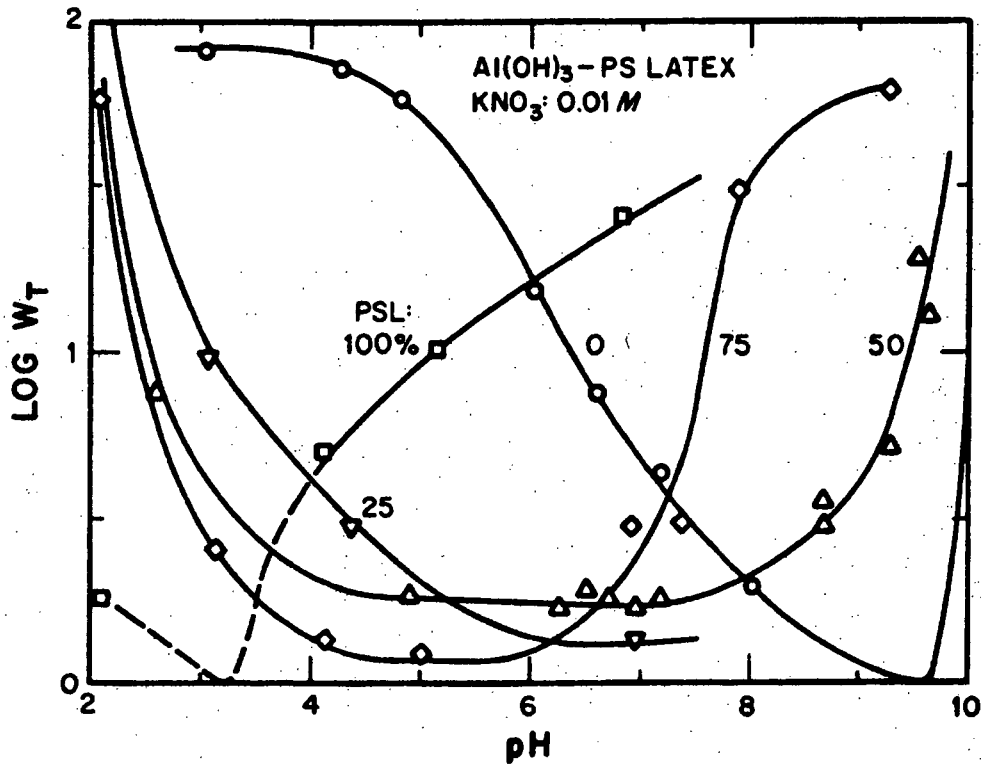


Fig. 10. Total stability ratio,  $W_T$ , as a function of pH for a pure aluminum hydroxide sol (Modal diameter 570 nm) (O), a pure polystyrene latex (PSL, modal diameter 380 nm) (□), and for mixtures of the two sols containing 25% (∇), 50% (Δ) and 75% (◇) PSL particles (in terms of number concentration).

C-2

As seen in Figure 10, the latex is least stable at low pH ( $\sim 3$ ) whereas pure aluminum hydroxide is unstable at high pH ( $\sim 9.5$ ). These pH values are close to the isoelectric points of the two colloidal systems. Depending on the particle number ratio and pH the binary systems may be either less or more stable than individual sols. For example, at pH 6 all mixed dispersions are less stable than the single systems. This is understood if one considers that the particles of PSL and of aluminum hydroxide carry opposite charges. At pH 8 the system containing 25% aluminum hydroxide particles is more stable than the pure aluminum hydroxide sol. In the studied case, aluminum hydroxide sol was carefully washed to eliminate all sulfate ions which are present in the particles as they are prepared (4).

Figure 11 gives an analogous plot to the previous one except that the aluminum hydroxide particles still contained some sulfate ions. The difference in the behavior of the purified and unpurified aluminum hydroxide sol is quite dramatic. In addition, the reproducibility of the results in the latter case is rather poor. This study exemplifies the sensitivity of such systems to anionic contaminations which often tend to be disregarded.

#### Particle Adsorption

Mixed systems which contain particles greatly divergent in size cannot be analyzed in the same manner as those having particles of comparable size. In the former case, the more finely dispersed systems may coagulate selectively, a heterofloc may form, or the small particles may adsorb on the larger ones, causing a change in the properties of the latter. All of these phenomena were observed in a binary system containing negatively charged polyvinyl chloride (PVC) latex (particle diameter 1020 nm) and silica (diameter  $\sim 14$ nm). It was shown that under certain conditions silica adsorbs on latex enhancing its stability toward electrolytes (22).

ORIGINAL PAGE IS  
OF POOR QUALITY.

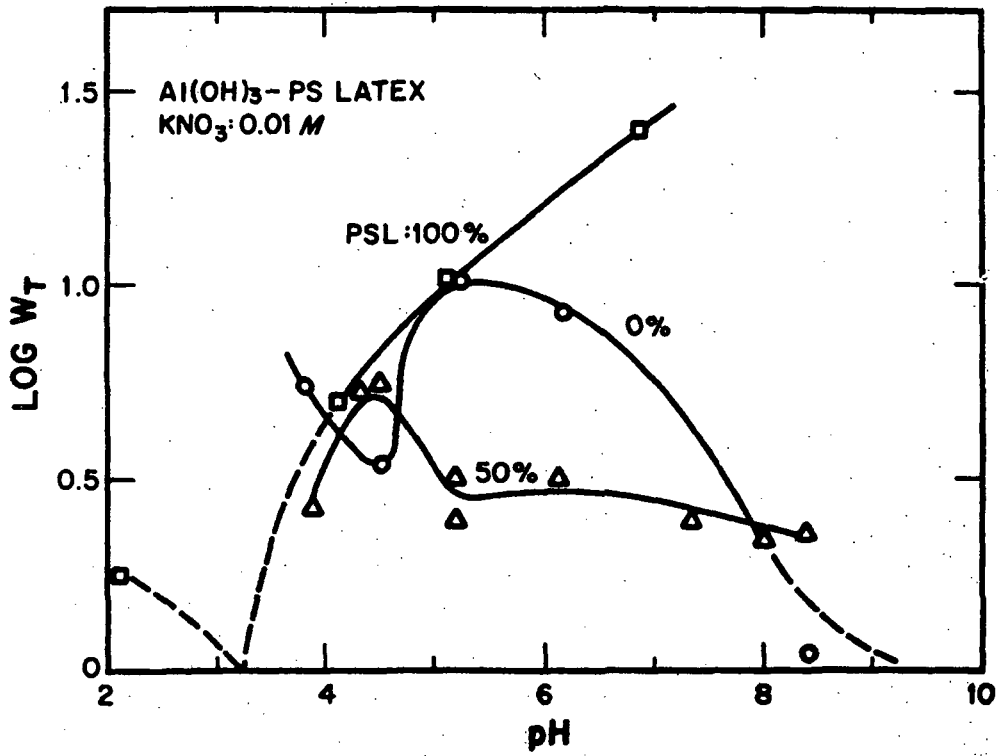


Fig. 11. Analogous plot as Figure 10 except that the aluminum hydroxide particles contained some sulfate ions.

The adsorption of small particles on larger ones is of particular interest, as other properties - in addition to stability - can be altered, such as the surface charge, reactivity, wettability, adhesivity, pigment characteristics, etc.

Figure 12 shows the mobility of a (PVC) latex as a function of pH and of the same latex in the presence of four different concentrations of  $\text{Fe}(\text{NO}_3)_3$ . In all cases the addition of the ferric salt had a strong effect on the particle charge causing the charge reversal from negative to positive at appropriate pH values. Independent measurements showed that the sharp change in the electrokinetic mobility was associated with the precipitation of ferric hydroxide. Consequently, the modification of the latex surface was due to the deposition of the metal hydrous oxide on the polymer particles. Needless to say the so coated latex showed different stability, adhesion characteristics, etc. than the untreated material.

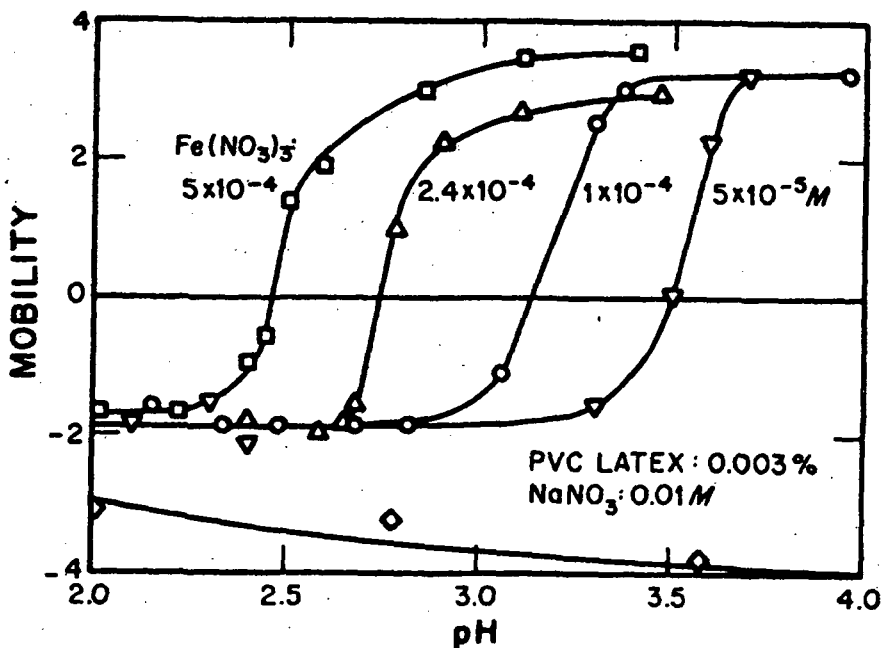


Fig. 12. Electrokinetic mobilities ( $\mu\text{m}/\text{sec}/\text{V}/\text{cm}$ ) as a function of pH of PVC latex (0.003% by wt, modal particle diameter 320 nm) in the absence ( $\diamond$ ) and in the presence of  $\text{Fe}(\text{NO}_3)_3$ :  $5 \times 10^{-5}$  ( $\nabla$ ),  $1 \times 10^{-4}$  (O),  $2.4 \times 10^{-4}$  ( $\Delta$ ), and  $5 \times 10^{-4}$  M ( $\square$ ).



It is expected that reactants which affect the precipitation of ferric hydroxide would also influence its interaction with the latex. This is clearly evident in Figure 13, which gives the mobility data of the same latex in the presence of  $\text{Fe}(\text{NO}_3)_3$  to which NaF was added in different concentrations. Fluoride ions are known to complex with the ferric ion and, as a result, the precipitation phenomena as well as the surface charge groups of ferric hydroxide are altered by these anions. Indeed, with increasing fluoride concentration the charge reversal occurs at higher pH values and the magnitude of the positive charge decreases.

Acidification of the sols containing particles with adsorbed metal oxides should bring about dissolution of the coating and, consequently, a change in the surface charge to less positive, or even negative. Figure 14 shows that in the presence of  $\text{HNO}_3$  and HCl very long times are needed to dissolve, at least in part, the metal oxide coating. However, even after one month the charge is not reversed back to negative; obviously, the metal hydrous oxide must be polymerized at the surface to which it adheres tightly. Addition of only 0.0010 M NaF greatly accelerates the removal of the oxide layer and the particles eventually become uncharged. The latter observation implies that the negatively charged potential determining groups of the original latex surface are neutralized by the metal counterion complexes. Apparently, the bonds formed between the stabilizing sulfate ions and the adsorbed ferric species are not broken by acidification even in the presence of  $\text{F}^-$ .

#### PARTICLE ADHESION

The deposition of colloidal particles on other solids and their removal from these substrates depend on the chemical and physical forces acting between the adhering surfaces. In the absence of chemical bonds the adhesion can be treated as heterocoagulation of dissimilar particles, taking the radius of one

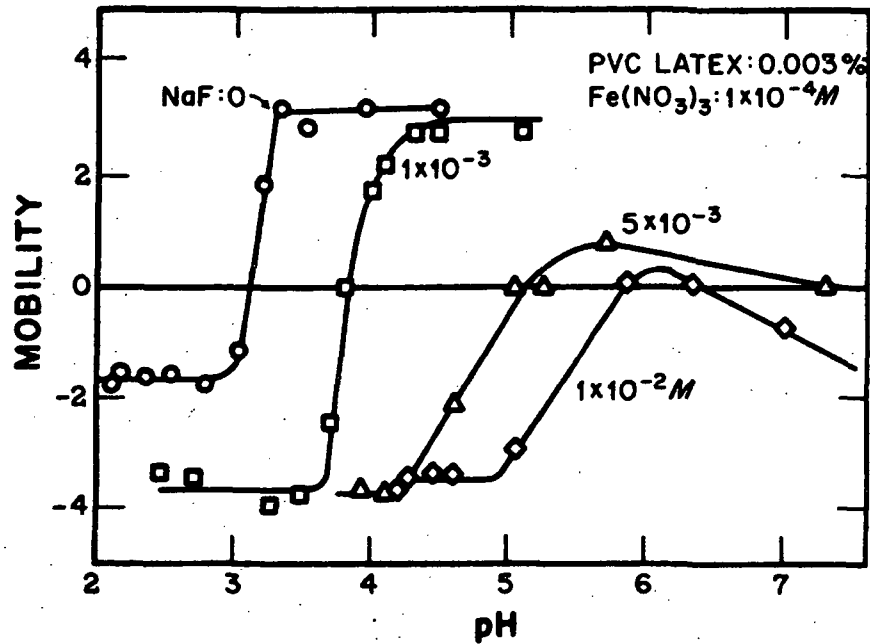


Fig. 13. Electrokinetic mobilities as a function of pH of the same PVC latex as in Figure 12 in the presence of  $1 \times 10^{-4}$  M  $\text{Fe}(\text{NO}_3)_3$  (○) to which  $1 \times 10^{-3}$  (◻),  $5 \times 10^{-3}$  (◻), and  $1 \times 10^{-2}$  M (◊) NaF was added, respectively.

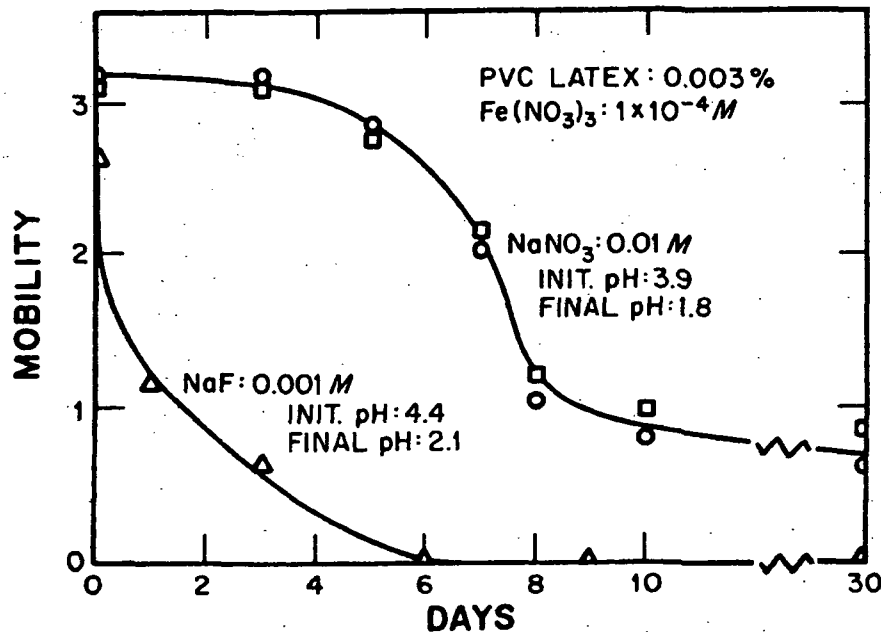


Fig. 14. The change of electrokinetic mobilities ( $\mu\text{m}/\text{sec}/\text{V}/\text{cm}$ ) as a function of time (days) of the same PVC latex as in Fig. 12 on acidification of a sol containing  $1 \times 10^{-4}$  M  $\text{Fe}(\text{NO}_3)_3$ . Circles and squares represent systems to which HCl and  $\text{HNO}_3$ , respectively, were added to lower the pH in the presence of 0.01 M  $\text{NaNO}_3$ ; triangles represent systems the pH of which was lowered by  $\text{HNO}_3$  in the presence of 0.0010 M NaF prior to aging.

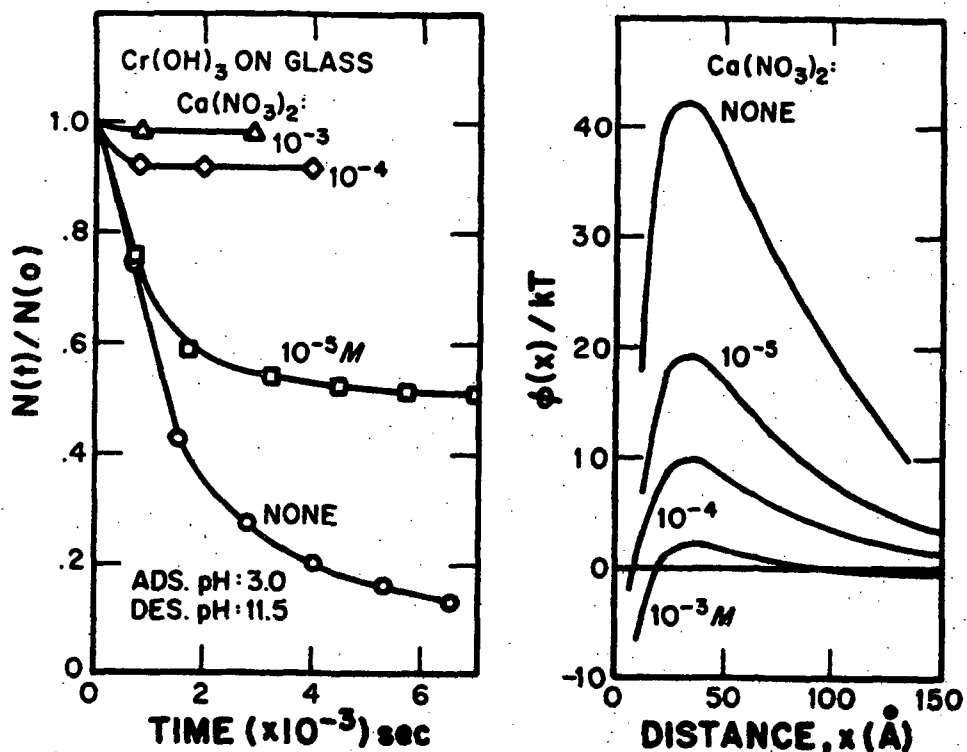


Fig. 15. Left: Fraction of monodispersed spherical chromium hydroxide particles (modal diameter 280 nm) desorbed from glass on repeated elution with rinse solutions of pH 11.5 in the absence (○) and in the presence of 10<sup>-5</sup> (◻), 10<sup>-4</sup> (◇), and 10<sup>-3</sup> M Ca(NO<sub>3</sub>)<sub>2</sub>. The particles were adsorbed on the glass from a sol at pH 3. Right: Calculated potential energy curves as a function of distance using the sphere-plate model (Eqs. 2 and 4) for the same systems shown left.

to go to infinity. In order to compare the theoretical predictions with experimental data it is necessary to have sufficiently well defined systems with known parameters. Again, monodispersed metal hydroxides, particularly those of spherical particles, can serve as excellent models for particle adhesion and removal studies. Using the packed column procedure (23), the interactions of such sols with glass and steel have been studied as a function of various conditions (pH, different electrolytes, temperature, etc.)

Figure 15 illustrates the results obtained with spherical chromium hydroxide particles (diameter 280 nm) on glass (24). At pH 3 glass beads placed in a column rapidly and quantitatively remove these metal hydroxide particles from an aqueous suspension by adhesion. Under these conditions the sol is positively charged and stable whereas the glass beads are negatively charged. Precautions are taken that no filtration takes place in the course of the deposition process. The subsequent removal of particles depends on the composition of the rinsing solution. At pH 11.5, at which both solids are negatively charged, rapid desorption of the particles is observed (Figure 15 left). However, if the rinse solution contains  $\text{Ca}(\text{NO}_3)_2$ , desorption can be reduced or completely inhibited depending on the concentration of the electrolyte. The higher the charge of the added cation, the lower is the concentration needed to prevent particle removal (24).

The results can be interpreted in terms of the total interaction energies. The attractive energy,  $\phi_A$ , as a function of distance ( $x$ ) was calculated using the equation:

$$\phi_A(x) = \frac{A_{132}}{6} \left[ \frac{2a(x+a)}{x(x+2a)} - \ln \frac{x+2a}{x} \right] \quad (2)$$

$A_{132}$  is the overall Hamaker constant for the system sphere-medium-plate, which can be approximated by:

$$A_{132} \approx (\sqrt{A_{11}} - \sqrt{A_{33}}) (\sqrt{A_{22}} - \sqrt{A_{33}}), \quad (3)$$

where subscript 1 applies to chromium hydroxide, 2 to glass, and 3 to water.

The value  $A_{11}$  for chromium hydroxide was taken as 14.9 kT,  $A_{22}$  for glass as 20.9 kT, and  $A_{33}$  for water as 10.3 kT.

For double layer repulsive energy,  $\phi_R$ , the plate/sphere expression of Hogg, Healy and Fuerstenau (25) was taken:

$$\phi_R(x) = \frac{\epsilon a}{4} \left[ (\psi_1 + \psi_2)^2 \ln(1 - e^{-\kappa x}) + (\psi_1 - \psi_2)^2 \ln(1 - e^{-\kappa x}) \right] \quad (4)$$

in which  $\psi_1$  and  $\psi_2$  are the surface potentials (equated with the corresponding  $\zeta$ -potentials), for the plate and the particles, respectively,  $\epsilon$  is the dielectric constant, and  $\kappa$  the reciprocal Debye-Hückel thickness.

The right side of Figure 15 gives the calculated total interaction energy curves,  $\phi(x) = \phi_A(x) + \phi_R(x)$ , as a function of distance of separation for the chromium hydroxide/glass systems in the absence and in the presence of the same concentrations of  $\text{Ca}(\text{NO}_3)_2$  as used in the desorption experiments. At the highest salt concentration essentially only attraction prevails and indeed no particle removal is observed. When no calcium nitrate is added, a number of particles appears to be at sufficient distance which enables them to overcome the energy barrier and desorb; however, particles which escaped cannot re-adsorb due to the high potential barrier. Thus, the double layer theory, albeit in its oversimplified form, explains at least semiquantitatively the adhesion phenomena in the described system.

Similar observations were made with chromium hydroxide on steel (Figure 16). The reproducibility of data is best shown by triangles and squares which represent two separate runs made with beds of steel beads on which the number of originally adsorbed particles differed by nearly one order of magnitude.

ORIGINAL PAGE IS  
OF POOR QUALITY

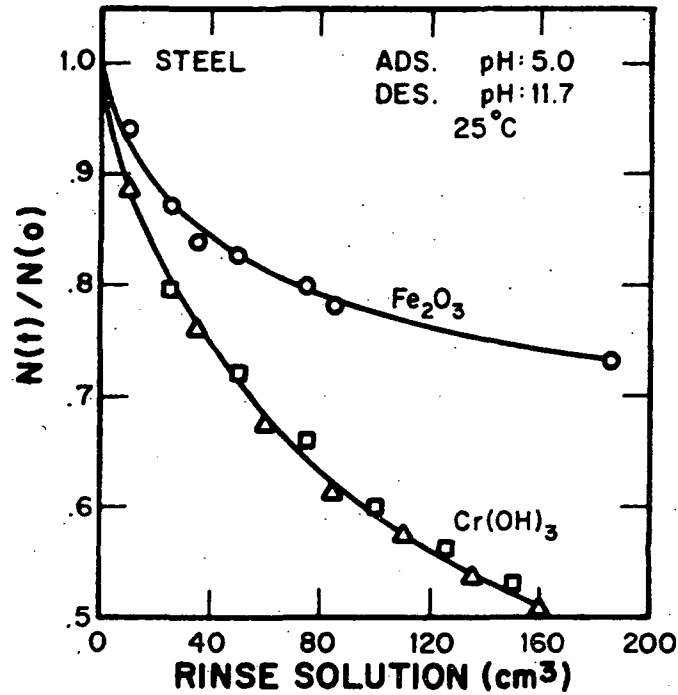


Fig. 16. Fraction of monodispersed spherical chromium hydroxide particles (modal diameter 280 nm) desorbed from steel on rinsing with an aqueous solution of pH 11.7. Number of particles originally deposited on 3 g of steel at pH 5.0 was  $2.9 \times 10^9$  ( $\square$ ) and  $1.8 \times 10^{10}$  ( $\triangle$ ). Circles give the analogous data for desorption of spherical hematite particles (modal diameter 140 nm) from the same steel. The number of originally deposited hematite particles:  $3.0 \times 10^9$ .

In the same diagram is also included the desorption curve of spherical hematite particles from the same steel under otherwise identical conditions. The large difference in the desorption rate is primarily due to the variation in the attractive forces, as determined by the Hamaker constants. This illustrates the sensitivity of the adhesion phenomena to the physical properties of the adsorbent/adsorbate system.

#### CONCLUDING REMARKS

It was not the intention of this review to give an in depth analysis of each problem discussed. Readers are referred to individually cited reports for more detailed information of the experimental techniques, the results obtained, and the theoretical analyses. However, it is hoped that the different cases described in this presentation clearly show the usefulness of the monodispersed metal hydroxide systems in the studies of various interfacial phenomena.

#### ACKNOWLEDGMENTS

This article is based on work done with the support of the NSF Grants CHE77 02185 and ENG 75-08403 as well as EPRI contract RP-966-1.

The author is greatly indebted to his many collaborators, and specifically to R. Brace, B. Gray, E. Katsanis, J. Kolakowski, H. Kumanomido, R. Kuo, J. Rubio, R. Sapiieszko, H. Sasaki, P. Scheiner, W. Scott, T. Sugimoto, and R. Wilhelmy, on whose contributions was based this presentation.

REFERENCES

1. E. Matijevic; Progr. Colloid Polymer Sci., 61 (1976) 24.
2. E. Matijevic and P. Scheiner, J. Colloid Interface Sci., 63 (1978) 509.
3. E. Matijevic; R. Sapiieszko and J. B. Melville, J. Colloid Interface Sci., 50 (1975) 567.
4. R. Brace and E. Matijevic; J. Inorg. Nucl. Chem., 35 (1973) 3691.
5. W. B. Scott and E. Matijevic; J. Colloid Interface Sci. (in press).
6. R. Demchak and E. Matijevic; J. Colloid Interface Sci., 31 (1969) 257.
7. E. Matijevic; A. D. Lindsay, S. Kratochvil, M. E. Jones, R. I. Larson and N. W. Cayey, J. Colloid Interface Sci., 36 (1971) 273.
8. P. McFadyen and E. Matijevic; J. Inorg. Nucl. Chem., 35 (1973) 1883.
9. E. Matijevic; M. Budnik and L. Meites, J. Colloid Interface Sci., 61 (1977) 302.
10. K. H. Lieser, Angew Chem., Int. Ed., 8 (1969) 188.
11. A. Bell and E. Matijevic; J. Inorg. Nucl. Chem., 37 (1975) 907.
12. A. Bell and E. Matijevic; J. Phys. Chem. 78 (1974) 2621.
13. R. S. Sapiieszko, R. C. Patel, and E. Matijevic; J. Phys. Chem., 81 (1977) 1061.
14. G. A. Parks, Chem. Rev., 65 (1965) 177.
15. M. Visca and E. Matijevic; J. Colloid Interface Sci. (in press).
16. T. Sugimoto and E. Matijevic; J. Inorg. Nucl. Chem. (in press).
17. P. H. Tewari and A. B. Campbell, J. Colloid Interface Sci., 55 (1976) 531.
18. Yu. F. Krupyanskii and I. P. Suzdalev, Sov. Phys.-JETP, 38 (1974) 859.
19. H. Kumanomido, R. C. Patel and E. Matijevic; J. Colloid Interface Sci. (in press).
20. J. Rubio and E. Matijevic; J. Colloid Interface Sci. (in press).
21. A. Bleier and E. Matijevic; J. Colloid Interface Sci., 55 (1976) 510.
22. A. Bleier and E. Matijevic; J. Chem. Soc., Faraday Trans. I, 74 (1978) 1346.
23. E. J. Clayfield and E. C. Lumb, Disc. Faraday Soc., 42 (1966) 285.
24. J. Kolakowski and E. Matijevic; J. Chem. Soc., Faraday Trans. I (in press).
25. R. Hogg, T. W. Healy and D. W. Fuerstenau, Trans. Faraday Soc., 62 (1966) 1638.